JCI insight

Systemic and adipocyte transcriptional and metabolic dysregulation in Idiopathic Intracranial Hypertension

Connar S.J. Westgate, … , Gareth G. Lavery, Alexandra J. Sinclair

JCI Insight. 2021. https://doi.org/10.1172/jci.insight.145346.

Clinical Medicine | In-Press Preview | Neuroscience | Ophthalmology

Graphical abstract

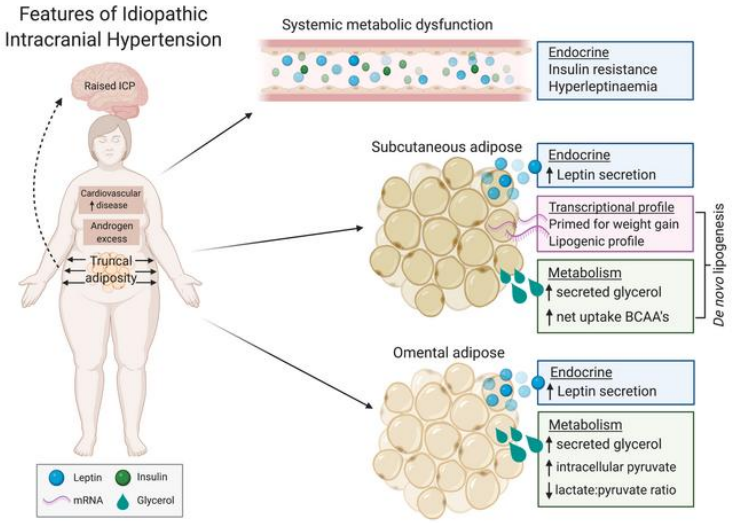

Find the latest version:

https://jci.me/145346/pdf

Systemic and adipocyte transcriptional and metabolic dysregulation in Idiopathic Intracranial Hypertension.

Connar SJ Westgate[1,2], Hannah F Botfield[3], Zerin Alimajstorovic[1,2], Andreas Yiangou[1,4], Mark Walsh[5], Gabrielle Smith[1,2], Rishi Singhal[6], James L Mitchell[1,2], Olivia Grech[1,2], Keira A Markey[1,4], Daniel Hebenstreit[5], Daniel A Tennant[1] , Jeremy W Tomlinson[7], Susan P Mollan[8], Christian Ludwig[1,2], Ildem Akerman,[1,2] Gareth G Lavery[1,2] and Alexandra J Sinclair[1,2,4*]

1. Institute of Metabolism and Systems Research, College of Medical and Dental Sciences, University of Birmingham, Birmingham, B15 2TT, United Kingdom (UK);
2. Centre for Endocrinology, Diabetes and Metabolism, Birmingham Health Partners, Birmingham, B15 2TH, UK;
3. Institute of Inflammation and Ageing, College of Medical and Dental Sciences, University of Birmingham, Birmingham, B15 2TT, UK;
4. Department of Neurology, University Hospitals Birmingham NHS Foundation Trust, Queen Elizabeth Hospital, Birmingham, B15 2WB, UK;
5. School of Life Sciences, University of Warwick, Coventry, UK;
6. Upper GI Unit and Minimally Invasive Unit, Heartlands Hospital, University Hospitals Birmingham NHS Foundation Trust, Birmingham B9 5SS, UK;
7. Oxford Centre for Diabetes, Endocrinology & Metabolism (OCDEM), NIHR Oxford Biomedical Research Centre, University of Oxford, Churchill Hospital, Headington, Oxford, OX3 7LJ, UK.
8. Birmingham Neuro-Ophthalmology, Ophthalmology Department, Queen Elizabeth Hospital, University Hospitals Birmingham NHS Foundation Trust, Birmingham, B15 2TH, UK

Corresponding author:* Alexandra Sinclair, Institute of Metabolism and Systems Research, College of Medical and Dental Sciences, University of Birmingham, Birmingham, B15 2TT, UK; a.b.sinclair@bham.ac.uk

Abstract

Background: Idiopathic intracranial hypertension (IIH) is a condition predominantly affecting obese women of reproductive age. Recent evidence suggests that IIH is a disease of metabolic dysregulation, androgen excess and an increased risk of cardiovascular morbidity. Here we evaluate systemic and adipose specific metabolic determinants of the IIH phenotype.

Methods: In fasted, matched IIH (N=97) and control (N=43) patients, we assessed: glucose and insulin homeostasis and leptin levels. Body composition was assessed along with an interrogation of adipose tissue function via nuclear magnetic resonance metabolomics and RNA sequencing in paired omental and subcutaneous biopsies in a case control study.

Results: We demonstrate an insulin and leptin resistant phenotype in IIH in excess to that driven by obesity. Adiposity in IIH is preferentially centripetal and is associated with increased disease activity and insulin resistance. IIH adipocytes appear transcriptionally and metabolically primed towards depot-specific lipogenesis.

Conclusions: These data show that IIH is a metabolic disorder in which adipose tissue dysfunction is a feature of the disease. Managing IIH as a metabolic disease could reduce disease morbidity and improving cardiovascular outcomes.

Funding: This study was supported by the National Institute of Health Research UK (NIHR-CS-011-028), the Medical Research Council UK (MR/K015184/1) and the Midlands Neuroscience Teaching and Research Fund.

Introduction

Idiopathic intracranial hypertension (IIH) is characterised by elevated intracranial pressure (ICP) and papilloedema typically manifesting as disabling daily headaches and visual disturbances which leads to permanent visual loss in up to 25% of patients (1–4). IIH predominantly occurs in obese women of reproductive age (greater than 90%), where incidence is increasing in line with the obesity epidemic (5). Consequently, IIH constitutes a substantial financial burden in the clinical setting (5). IIH incidence increases with rising body mass index (BMI), with disease activation often occurring following rapid weight gain (6, 7). Weight loss is therapeutic in IIH, with reduction in adiposity associated with reduction in ICP and improvements in headache and visual outcomes, suggesting a role of adipose tissue in IIH pathogenesis (8, 9).

The aetiology of IIH remains unclear, and an unmet research priority (10). IIH is no longer regarded as a disease isolated to the central nervous system as IIH patients have double the risk of cardiovascular disease (CVD) compared with obese individuals (6, 11). Importantly, IIH is a condition of androgen excess, and like in polycystic ovarian syndrome (PCOS) may contribute to cardio-metabolic diseases including T2D and CVD (12–14). We hypothesize that metabolic perturbations, possibly emanating from adipose tissue, contribute to the increased CVD risk in IIH.

In a large cohort of female IIH patients with active IIH, we assessed markers of systemic metabolic dysregulation and analyse adipose tissue distribution. We also aimed to identify underpinning molecular mechanisms through investigation of a unique cohort of IIH patients from which we investigated paired omental (OM) and subcutaneous (SC) adipose tissue function. Here we define the first detailed metabolic phenotype of IIH, and identify molecular mechanisms within adipose tissue that may contribute to CVD risk. We demonstrate that IIH patients have dysregulated systemic metabolism, in excess to that mediated by obesity, being more insulin resistant in the context of hyperleptinaemia and adipocyte leptin hypersecretion.

Furthermore, SC adipose would appear to be transcriptionally primed for increased calorie intake with a unique depot-specific lipogenic profile.

Results

Patient characteristics

Patients with active untreated IIH (97) and control patients (43) were prospectively recruited. The IIH cohort were all female, aged 32.4 ± 7.8 years and obese (BMI 40.0 ± 6.5 Kg/m^2), with raised lumbar puncture opening pressure (LP OP) (34.8 ± 5.7 cmCSF) and papilloedema. The control cohort were matched for BMI and gender but were older (**Table 1**). Baseline characteristics and characteristics of the sub-study cohorts can be found in **Table 1** and **supplemental figure 1**.

IIH patients have an insulin resistant phenotype

Epidemiological data has suggested that IIH patients have an increased risk of type 2 diabetes mellitus (T2D) and cardiovascular morbidity, suggestive of systemic metabolic dysfunction (6). Hence, we evaluated markers of insulin resistance in IIH. Fasting insulin levels were elevated in IIH (IIH 18.1 ± 13.3 mlU/L vs controls 12.1 ± 6.7 mlU/L Mann-Whitney U, U=1421, p=0.0025, **Fig 1B**), with markers of insulin resistance elevated in IIH compared to controls (Homeostatic Model assessment 2 Insulin resistance (HOMA2-IR), 1.97 ± 1.44 vs 1.33 ± 0.74; p=0.0030, **Fig 1C**), higher β-cell function in IIH (HOMA2-%B scores of 163.6 ± 76.4 vs 128.6 ± 48.7; p=0.0097, **Fig 1D**) and lower insulin sensitivity in IIH (HOMA2-%S scores of 72.4±45.5 vs 131.6±153.3; p=0.0030, **Fig 1E**), where these features are associated with a progression to T2D (15). Additionally, a higher proportion of IIH patients have insulin resistance, as defined by a HOMA2-IR>1.8, (IIH 47.5% vs controls 22.6%; p=0.0155, Fisher's exact test) (16). Given that the control cohort is older than the IIH cohort, a multiple regression analysis was carried out on the HOMA2-IR results, taking both age and BMI into consideration. This analysis demonstrated that IIH patients had higher levels of insulin resistance (1.89±0.28 vs 1.51±0.26 HOMA2-IR; p<0.0001, **Fig S2**). The fasting glucose (**Fig 1A**) and glycated haemoglobin (HbA1c) (**Fig 1F**) levels were comparable between IIH and control subjects, despite the controls being older. The relationship between insulin resistance and IIH disease activity,

inferred from the ICP, was evaluated, where the relationship between (LP OP and HOMA2-IR was weak (p=0.051, correlation coefficient (ρ)=0.12).

We evaluated the lipid profile in IIH, a risk factor for cardiovascular morbidity (17). We demonstrate no differences in IIH fasted cholesterol (IIH 4.94 ± 0.91 vs controls 5.09±0.95 mmol/L, t-test, $t_{(133)=}$0.88, p=0.37, **Fig 1G**) and triglycerides (IIH 1.54 ± 1.01 vs controls 1.42 ± 0.60 mmol/L, Mann-Whitney, U=1889, p=0.96, **Fig 1H**) compared to the controls. We also evaluated hepatic and renal function in the IIH and control subjects **(Sub-study 1, table 1)** and noted a number of differences in IIH, although levels remained within the normal clinical reference range.

Obesity in IIH

It is well established that adipose distribution is a determinant of insulin resistance and cardiovascular risk (18, 19). Given that our data demonstrates a greater degree of insulin resistance, we assessed the adipose distribution and lean mass in IIH patients (**Sub-study 2**,**table 1**) (20). We determined that IIH patients have a similar total mass, fat mass and lean mass compared to control patients. However, when assessing the truncal region, the adipose depot most associated with metabolic risk and insulin resistance, we demonstrate increased fat (IIH 46.03±6.29 vs controls 42.66 ± 5.84 %, t-test, $t_{(52)}$=2.037, p=0.046, **Fig 2A**) and lower truncal lean mass (IIH 52.27 ± 6.15 vs controls 55.97 ± 5.64 %, t-test, $t_{(52)}$=2.304, p=0.025, **Fig 2B**) in IIH. Accordingly, there is an increased truncal fat to lean mass ratio in IIH patients (0.94 ± 0.30 vs 0.78 ± 0.19, Mann-Whitney U, U=24, p=0.0441; **Fig 2C**). No differences in limb fat (**Fig 2D**) and lean mass (**Fig 2E**) suggests preferential truncal adipose deposition in IIH.

Obesity is associated with insulin resistance and intracranial pressure

Previous work demonstrated that truncal adiposity correlates with LP OP in IIH, suggesting that adiposity is associated with IIH disease activity (8). In this larger IIH cohort we recapitulate this finding, demonstrating that LP OP correlated with total (p=0.016, ρ=0.37, **Fig 2F**) and truncal fat mass (p=0.035, ρ=0.31, **Fig 2G**). Total adipose mass is strongly associated with

insulin resistance in obese individuals, and is observed in the present IIH cohort, linking excess abdominal adiposity to insulin resistance in the IIH patients (p=0.0017, ρ=0.46, **Fig 2H**) (20).

IIH patients have comparative hyperleptinaemia

The satiety adipokine leptin is strongly associated with obesity, insulin resistance and metabolic dysfunction, and has been proposed to be pathogenic in IIH (21, 22). Interpretation of previous leptin studies in IIH is limited by sample size, selection of the control cohorts and variable fasting status (21, 23–26). Here we compared both serum and CSF in IIH patients against a healthy control cohort to determine if leptin is altered, and assessed the relationship of leptin to markers of metabolic dysfunction.

In the study cohort, we demonstrate elevated fasted serum leptin (IIH, 79.5±30.4 vs controls 63.5 ± 14.9 ng/ml, Welch's t-test $t_{(63.09)}$=3.059; p=0.003 **Fig 3A**) in IIH patents compared to patients with obesity (matched gender and BMI (**Fig S1**)). A further sensitivity analysis, additionally matching the controls for age as well as gender and BMI, confirms raised serum leptin (IIH, 75.6 ± 30.4 vs controls, 63.5 ± 14.9, Welch's test, $t_{(59.20)}$=2.089, p=0.04, **Fig S3A**). This demonstrates that IIH patients have hyperleptinaemia in excess to that observed in obesity (27). Transport of leptin into the CNS is saturable at higher levels of serum leptin in obesity (28). In keeping with this there were no differences in CSF and serum/CSF ratio between IIH and control subjects (**Fig 3B, C** and **Fig S3B and C**). It is unlikely that hyperleptinaemia is driving disordered CSF dynamics in IIH as neither serum (**Fig 3D**) or CSF (**Fig 3E**) leptin levels correlated with LP OP in IIH.

IIH hyperleptinaemia is likely a reflection of systemic metabolic dysregulation in IIH. We note that body fat percentage positively correlates with serum leptin in IIH patients (p<0.0001, r=0.74) as it does in obesity (28). Additionally, elevated serum leptin is known to impact β-cell function in obesity and in keeping with this, serum leptin is associated with β-cell function in IIH (HOMA-%B, p=0.029, r=0.33) (29).

Assessment of paired subcutaneous and omental adipose tissue

We show that adiposity, is associated with LP OP, a reflection of IIH disease activity (**Fig 2**). Loss of adiposity is disease modifying in IIH (8, 9). We have also demonstrated hyperleptinaemia in IIH in excess of that driven by obesity (**Fig 3**). In obesity, these factors are associated with disordered adipose tissue metabolism (27). Consequently, we hypothesised that in IIH, adipose tissue would display perturbed function and metabolism, in excess to that expected from obesity alone. In order to examine our hypothesis in detail we recruited IIH and control subjects undergoing bariatric surgery and collected matched abdominal subcutaneous and omental adipose tissue biopsies (patients matched for age, gender and BMI **Fig S4**) and conducted a series of *in vitro*, molecular and metabolic assessments to examine phenotype.

Subcutaneous and omental tissue morphology

Histomorphometric analysis compared adipose tissue (SC and OM adipose depots) between IIH and control subjects (matched age, gender and BMI **Fig S4**). IIH SC adipocytes (**Fig 4C**) had a similar cross sectional area compared to controls, with a similar distribution of adipocyte area (**Fig 4D**). However, IIH OM adipocytes are smaller than controls (IIH, 3286±176 vs controls, 4056 ± 342 μm^2; $t_{(16)}$=2.206, P=0.042; **Fig 4E**). In particular there was an increased frequency of adipocytes at an area of 1000μm^2 (IIH 8.8 ± 1.7 vs controls 2.7 ± 1.2%; p<0.01) and at 2000μm^2 (IIH 27.9 ± 2.6 vs controls 17.2 ± 3.9%; P<0.0001; **Fig 4F**) indicating an increased proportion of small adipocytes (ordinary two-way ANOVA followed by Sidak's test, Row factor $F_{(17,288)}$=87.82, p<0.0001).

Adipocyte leptin hypersecretion in IIH

We showed in **Fig 3** that IIH is a state of hyperleptinaemia. Consequently, we assessed leptin secretion in *ex vivo* adipose tissue (IIH compared to matched controls, **Fig S4**) to determine if adipose leptin hypersecretion is contributing to the enhanced hyperleptinaemia. Consistent with the systemic data, we demonstrated that both SC (IIH 8.3 ± 1.6 vs controls 2.4 ± 0.4

ng/ml/100mg; Welch's test; $t_{(11.47)}$=3.6; P=0.0039, **Fig 5A**), and OM (IIH 2.9±0.8 vs controls 0.6 ± 0.1 ng/ml/100mg; Welch's test; $t_{(9.276)}$=2.917; P=0.016, **Fig 5B**) adipose tissue from IIH patients secretes more leptin compared to BMI matched controls. Although adipose leptin secretion is elevated in IIH, this is independent of gene expression (Ob gene (leptin) from RNA sequencing) (**Fig 5C**) and adipocyte size (**Fig 4**).

IIH adipose tissue is transcriptionally primed for lipid accumulation

We examined the transcriptional profile of SC adipose tissue in IIH patients compared to a control cohort matched for gender and BMI (**Figure S4**). RNA sequencing followed by differential gene expression analysis revealed 708 up-regulated and 696 down-regulated Refseq genes in IIH SC adipose tissue, based on p-values <0.05 (**Fig 6A**) where the genes can be found in supplemental spreadsheet 1.

In order to identify signatures unique to IIH SC tissue we performed gene ontology analysis using DAVID (**Fig 6C**), where gene lists and statistics can be found in supplemental spreadsheet 2. Our analysis did not reveal gene pathways enriched in upregulated genes but revealed gene pathways prominently enriched in downregulated genes. Our results suggested that the enrichment for these pathways was mainly driven by the strongly downregulated ribosomal genes. Previous reports have linked suppression of the highly expressed rDNA gene transcription (ribosomal genes) as a prerequisite to lipid accumulation and energy storage (30–32). Therefore, we specifically interrogated ribosomal subunit genes (33), highly expressed genes as well as gene sets regulated by caloric intake (34) and lipid biosynthesis for enrichment in IIH SC using GSEA gene ontology analysis (Figure 6 C, D). We find that in IIH SC, ribosomal genes are repressed, suggesting active energy storage (Fig 6 D). Moreover, IIH SC transcriptional profile was enriched for gene expression changes associated with caloric intake during lipid biosynthesis (Figure 6 F,G,). Both IIH SC and control SC are derived from patients who have undergone an overnight fasting (routine before surgery), thus gene expression profile in IIH SC consistent with caloric intake and active lipidogenesis is unexpected. Taken together, SC adipose tissue in IIH patients displays a transcriptional

profile consistent with active lipogenesis, despite the lack of caloric intake, suggesting an uncoupling of lipidogenesis from actual caloric intake.

IIH adipocytes have perturbed metabolism

Given our findings of elevated levels of insulin resistance in IIH and the demonstration that genes associated with lipogenesis are upregulated in SC adipose tissue **(Fig 6)** we conducted non-targeted NMR metabolomics to provide insight into the metabolism of the IIH tissue compared to matched controls (**Fig S4**). NMR spectra analysis allowed identification of 29 metabolites in explant cultured SC and OM adipose tissue (**Table S1**) and 34 metabolites in the respective culture media (**Table S2**).

IIH SC adipose tissue secreted more glycerol compared to controls (inferred from media incubated with adipose tissue relative to media without adipose tissue added, IIH 157.3 ± 62.6 vs controls 84.5 ± 37.0 ΔμM/100mg; Unpaired two-tailed t-test, $t_{(18)}$=3.168, P=0.0053, **Fig 7B**). There was no difference in intracellular glycerol (**Fig 7A**), and therefore an increase in the secreted/intracellular glycerol ratio (0.58 ± 0.43 vs 0.27±0.16; Mann Whitney test, U=14, p=0.0052, **Fig 7C**), an indication of enhanced glycerol secretion. Similarly, IIH OM adipose tissue secreted more glycerol compared to controls (128.7±45.7 vs 79.4±33.6 ΔμM/100mg; unpaired t-test, $t_{(17)}$=2.655, p=0.018, **Fig 7E**), without any alteration in intracellular glycerol (**Fig 7D**) and an increase in secreted/intracellular glycerol ratio (0.50 ± 0.18 vs 0.27 ± 0.11; unpaired two tailed t-test, $t_{(17)}$=3.243, p=0.0045, **Fig 7F**).

We additionally detected alterations in branch chained amino acid (BCAA) consumption, where the BCAAs, leucine and isoleucine, may be preferentially catabolised to lipogenic acetyl-CoA as previously shown to occur in adipocytes (35, 36). IIH SC adipose tissue displayed net uptake of both leucine (inferred from media incubated with adipose tissue relative to media without adipose tissue added, IIH -38.02 ± 40.76 vs control 22.62 ± 54.25 ΔμM/100mg; t-test, $t_{(18)}$=2.826, p=0.011, **Fig 7H**) and isoleucine (IIH -30.22 ± 25.21 vs controls 25.31 ± 48.26 ΔμM/100mg; Mann Whitney test, U=12, p=0.002) although adipose

intracellular isoleucine and leucine levels were not altered (**Fig 7G, I**). We suggest that IIH SC adipose tissue could be catabolising these amino acids to support *de novo* lipogenesis. Conversely, IIH OM adipose showed no difference in uptake or intracellular isoleucine and leucine (**Fig 7K-N**).

IIH OM adipose had elevated tissue pyruvate (23.63 ± 16.77 vs 4.58 ± 7.18 µM/100mg; Mann Whitney Test, U=13, p=0.0039, **Fig 8D**) with no change in tissue lactate (**Fig 8E**) and thus a decreased lactate to pyruvate ratio (145.0 ± 200 vs 544.9 ± 380.7; Mann Whitney Test, U=18, P=0.015, **Fig 8F**). We also show reduced uptake of pyruvate into the OM adipose (-226.1 ± 100.0 vs -344.0 ± 101.7 ΔµM/100mg; T-test, $t_{(17)}$=2.545, p=0.0209, **Fig 8I**) suggestive of reduced tissue pyruvate consumption. No difference in lactate secretion was detected between the groups. In parallel, a reduction in tissue acetate was observed in the IIH OM adipose alongside reduced secretion in the same depot (166.5±75.22 vs 286.8±64.85 µM/100mg; T-test, $t_{(18)}$=3.829, p=0.0012, **Fig 8M** and 335.4±176.4 vs 800.9±414.6 ΔµM/100mg; T-test, $t_{(17)}$=3.247, **Fig 8N**). No differences were observed in the SC adipose depot.

Discussion

IIH is a disease of elevated ICP predominantly amongst young women with obesity, where incidence is rising in line with global obesity trends. Epidemiological data has highlighted an increased risk of CVD in IIH in excess of that for obesity (6, 11). IIH has classically been regarded as a neuro-ophthalmic disease manifesting with headaches and risk of visual loss. Here, we provide the first evidence that IIH is a disease of systemic metabolic dysregulation with neuro-ophthalmic manifestations. The insulin resistance phenotype in IIH is congruent with the previously described androgen excess phenotype in IIH, where female androgen excess is linked to insulin resistance and T2D (14). Although our relatively young IIH cohort (mean age 32) does not meet the criteria for prediabetes, the presence of insulin resistance in 50% of the cohort as assessed by HOMAR-IR, coupled with altered β-cell function (HOMA B) indicates a risk for progression to prediabetes and T2D, particularly in later life. This has important clinical implications for patient care, as insulin resistance is a potentially modifiable risk factor for future cardiometabolic morbidity (37).

IIH patients have hyperleptinaemia in excess of obese controls and endorsed by elevated adipose leptin secretion. Previous studies also demonstrated raised serum leptin in IIH, where leptin was proposed to be causative in raised ICP (21). However, the lack of elevated CSF leptin and no correlation between leptin and LP OP suggests that hyperleptinaemia is unlikely to be directly driving disordered CSF secretion in IIH patients. Rather, we suggest that hyperleptinaemia is a feature of systemic metabolic perturbation. Hyperleptinaemia is a feature of other metabolic conditions and is associated with systemic insulin resistance, where insulin is a known leptin secretagogue (38, 39).

The relationship of the systemic metabolic perturbations in IIH to ICP dynamics and disease activity remains unclear. This study did not evaluate if the metabolic dysfunction was driving raised ICP and this requires further investigation. The metabolic phenotype in IIH does, however, provide compelling evidence that IIH is not merely a disease of the central nervous

system and eyes but a systemic metabolic disease. These metabolic features may be relevant to the previously documented, heightened CVD risk in IIH (6).

Obesity is a feature of metabolic disease, associated with insulin resistance and hyperleptinaemia (40). Supporting the hypothesis that IIH is a disorder of systemic metabolic dysregulation we noted increased truncal adiposity, which correlates with ICP, insulin resistance and hyperleptinaemia. Crucially, we show that IIH patients have a greater proportion of truncal fat to lean mass, where excess fat mass is associated with insulin resistance (41).

Truncal adiposity correlates with LP OP, a marker of IIH disease activity, this suggests that adiposity could be associated with disease activity. In support of this, previous studies have described reduction of truncal fat mass in association with disease remission (8, 9). It is however unknown if weight loss confers improvement of the metabolic phenotype in IIH. We were able to access a cohort of IIH SC and OM IIH tissue despite its scarcity, providing the invaluable opportunity to perform in depth analysis. We identified that IIH SC adipose displays a transcriptional profile consistent with active lipid biosynthesis following calorie intake, notable as both patients and controls were fasted at the time of the biopsy (30, 34). As such, these findings suggest that SC adipose tissue is geared for lipogenesis. We noted downregulation of highly expressed ribosomal genes. This is in keeping with previous literature demonstrating that during active lipogenesis, adipose tissue down-regulates the transcription of highly expressed genes (such as ribosomal genes) (34). Our metabolomic data suggests IIH adipose metabolism is dysregulated compared to control obese adipose. SC IIH adipose shows increased capacity for uptake of branch chain amino acids (BCAA), where isoleucine and leucine catabolism could contribute up to a quarter of the lipogenic acetyl-CoA pool (35). These data propose that IIH SC adipose tissue can preferentially catabolise BCAAs to support increased lipogenesis, corroborating the transcriptomic data (34). Given the indicators of increased lipogenesis, the elevated glycerol secretion from IIH adipocytes is unlikely to be derived from lipolysis. It is therefore possible that in-keeping with previous

studies, and the insulin resistant phenotype we have noted in IIH, the increased glycerol secretion could reflect breakdown of excess glucose through glyceroneogenesis within the SC adipose tissue (42).

Together these data could indicate that IIH patients are predisposed to gaining adipose mass, which is important to consider when IIH patients often experience an exacerbation or onset of symptoms following rapid weight gain (7, 43). Dynamic assessment of *de novo* lipogenesis in IIH SC adipose would help support this hypothesis.

In OM adipose tissue we identified decreased pyruvate uptake coupled with increased tissue levels of pyruvate. This is in the context of unchanged tissue and media lactate levels suggesting this is not occurring due to sensitivity to hypoxia, but more likely a means of the cell maintaining favourable cytosolic redox homeostasis under challenging metabolic conditions. This is however occurring in the setting of reduced tissue acetate and acetate secretion. Taken together our novel tissue approach has revealed that in IIH the OM depot maintains a more efficient energy network whilst the SC depot shows more signs of metabolic dysfunction potentially contributing to disease pathophysiology and cardiovascular risk.

The study findings are limited to adult women, rather than male (5% of IIH) or paediatric patients with IIH (5). By nature of the disease being prevalent during child bearing years, the cohort is relatively young and consequently further studies are now warranted to evaluate metabolic implications for a more aged IIH population where metabolic complications may be more severe. Our studies have found evidence of metabolic dysfunction compared to obesity despite a young age compared to controls (44). The typical young age of IIH patients is important as earlier intervention to modify cardiometabolic risk factors is likely to improve future mortality and morbidity from cardiovascular disease as seen in other conditions characterised by metabolic dysfunction (45, 46). The present study utilises a relatively small sample size compared other studies that assess more common diseases. Additionally our adipose tissue studies were powered based on previous similar studies, we however cannot

eliminate the possibility of larger sample sizes yielding different results. However, the data was strengthened by the detailed clinical phenotyping, as well as the notable number of IIH subjects considering that IIH is a rare disease. The results lay the foundation for a prospective in-depth metabolic assessment across the IIH life course.

We provide the first description of detailed metabolic phenotyping in active IIH, defining contributions to cardiovascular risk and identifying adipose tissue mechanisms that may contribute to pathophysiology (**Fig 9**). Adiposity in IIH is preferentially truncal with SC adipocytes demonstrating increased leptin secretion and transcriptional priming for caloric storage and gaining adipose mass. We also note differential fuel utilisation in the OM adipose. The adipose phenotype described maybe contributing to insulin resistance and will need further evaluation. These data indicate that IIH is likely a systemic metabolic disease with neuro-ophthalmic features rather than solely a neuro-ophthalmological disease. We have not determined the causal relationship between the metabolic derangement and intracranial pressure dysregulation in IIH and this would be worthy of future investigation. The metabolic phenotype is likely to explain the increased risk of cardiovascular disease and T2D in IIH. As IIH presents in early adulthood, modifying the metabolic aspects of the disease through addressing insulin resistance and managing cardiovascular risk factors, could improve patient long term outcomes.

Methods

Unless otherwise stated, materials are from Sigma-Aldrich, Poole, UK.

Study Design

A case control study comparing IIH with matched controls was conducted to assess the systemic metabolic profile: BMI, blood pressure, fasting glucose and insulin, cholesterol and triglycerides and leptin (serum and CSF). Sub-study 1 evaluated the hepatic and renal profile and sub-study 2 evaluated the body composition and distribution (Figure 1 supplemental). Adipose tissue was then evaluated in separate IIH and control populations.

Study population

Young (16-55) female IIH patients with active IIH (papilloedema > grade 1 Frisen and LP opening pressure > 25cmCSF on the date of research assessment visit) were recruited. The clinical consequences of IIH were not evaluated in this study, rather underling systemic disease activity was assessed; hence IIH patients at any stage of disease were included in the present analysis given that they had active disease. Patients who had previously failed pharmacotherapy, undergoing pharmacotherapy (such as acetazolamide) or failed community weight management were included in the study given the presence of active IIH, thus the IIH cohort represents a cohort with active disease. Control patients met the same inclusion criteria as the IIH patients, where absence of IIH was confirmed. The control subject cohort was matched to the IIH population for age, gender and BMI. Gender was participant reported.

Exclusion criteria

Exclusion criteria for all patients included receiving hormone manipulating medication, significant comorbidities including known endocrinopathies and the inability to give informed consent. Additionally, IIH patients were excluded if they were pregnant during the visit.

Assessments

All participants underwent detailed medical history and examination. All blood samples were collected following an overnight fast (from midnight). Lumbar punctures were carried out in all IIH patients and conducted in the left lateral decubitus with knees bent at a 90° angle or more and lumbar puncture opening pressure (LP OP) recorded before CSF was collected (up to 15ml). Serum samples not analyzed immediately were centrifuged (10 minutes at 1500 g at 4°C) aliquoted and stored at -80 °C. Cerebrospinal fluid (CSF) samples were centrifuged (800 g for 10 minutes at 4°C) and the supernatant was aliquoted and stored at -80 °C. All samples processed only underwent a single freeze-thaw cycle.

Clinical and biochemical analysis

BMI was calculated from weight and height and using the following formula: BMI = (weight (kg) / height $(m)^2$). Fasting glucose, glycated haemoglobin (Hb1Ac) and lipids were measured. In sub-study 1 subjects also had liver function (bilirubin, alkaline phosphatase (ALP) and aspartate amino transferase (AST)) and renal function tests (urea, creatinine and estimated glomerular filtration rate (eGFR) was calculated using the Chronic Kidney Disease Epidemiology collaboration (CDK-EPI) equation). All tests were conducted in the biochemistry department at University Hospital Birmingham NHS Foundation Trust, UK.

Fasting insulin and HOMA2-IR

Fasting insulin was measured using commercially available assays (Mercodia, Uppsala, Sweden), according to the manufacturer's instructions. Homeostasis model assessment of insulin resistance (HOMA2-IR) was calculated using the program HOMA calculator v2.2.3(www.dtu.ox.ac.uk/homacalculator).

Body composition

Duel energy x-ray absorptiometry (DEXA) was performed using a total-body scanner (QDR 4500; Hologic, Bedford, MA, USA), as previously described (20, 47) on a sub set of patients. The scans were conducted by a clinical scientist and trained radiographer. Patients with metal prosthetics or implants were included, and tissue overlying the prosthesis was excluded from analysis. Scans were checked for accuracy of fields of measurement. Regional fat mass was analysed as described previously (20, 47). The precision of total fat mass measures in terms

of coefficients of variation (CV) was less than 3%, and for regional fat analyses it was less than 5%. Both the IIH and control cohorts were analysed on the same DEXA scanner. Additionally, a subset of patients had body fat percentage determined by bio-impedance via a Body Composition Analyser TANITA BC-418 MA. A 0.2kg correction was made for base layer clothing where a standard female body type pre-set was selected for all patients. The machine was used according to manufacturer's instructions.

Adipose tissue collection

Adipose tissue from IIH patients was covered under the following ethical approvals (13/YH/0366 and 14/WM/0011). Bariatric control patients were identified from elective bariatric lists at Birmingham Heartlands Hospital NHS Trust who had no endocrinopathies and not on hormonal treatments under the following ethics approval (14/WM/0011). All patients were fasted overnight (from midnight) prior to adipose tissue biopsy. Adipose tissue (abdominal subcutaneous (SC)) and where possible omental (OM)) was biopsied and was either placed immediately in RNA later, into phenol free DMEM/F12 (Thermofisher, Paisley) without, UK antibiotics, or 4% formaldehyde.

Histomorphometric analysis

Adipose tissue was fixed in 4% formaldehyde prior to dehydration, clearing and embedding in paraffin wax. Embedded tissue was cut in 5 µm sections prior to a haematoxylin and eosin (H&E) stain. Sections were imaged using a Leica DM ILM inverted microscope (Leica Microsystems UK Ltd, Milton Keynes, UK) though a Leica DFC290 camera (Leica) utilising the Leica application suite (V2.8.1, Leica). Adipocyte area was assessed via the Image J (National Institutes of Health, Bethesda, MD) plugin Adiposoft (48). The evaluator was blinded to tissue type and patient disease state during analysis.

RNA sequencing

Stranded mRNA cDNA libraries derived from SC adipose tissue (insufficient omental tissues precluded this analysis) were sequenced at 2X100 paired end reads on the Illumina HiSeq 2500 platform (Illumina, San Diego, CA) by Eurofins Genomics. Control and IIH RNA had

comparable RNA integrity numbers quality (7.5 ± 0.82 vs. 7.7 ± 0.50, P=0.6), indicating suitable RNA integrity.

Quality control on the RNA sequencing was performed with FastQC v0.11.4. Read and adapter trimming was carried out using TrimGalore! v0.4.4 with Cutadept v1.13 with default settings (49). RNA-seq reads were mapped to the human genome (hg19, UCSC annotation) utilising STAR software v2.5.3a with default parameters (50). Counts per gene were calculated using custom scripts acting in a HTSeqcount compatible mode with the following parameters: --format=bam --minaqual=10 --stranded=reverse –mode=union (51, 52). Differentially expressed genes were identified using the DESeq2 (v1.14.1) from Bioconductor release 3.3 (53). Differentially expressed genes were called at a false discovery rate of 5%. Normalised FPKM values for each gene were calculated using DESeq2 and GenomicFeatures v1.26.4 package (54). Gene set enrichment analysis was carried out as described previously described (55, 56). Interrogated gene sets can be found in supplemental spreadsheet 3,where gene sets were derived from the following articles (30, 33, 34).

Data availability

The accession code for RNA sequencing data is GEO database: GSE171398.

Conditioned media protocol

Adipose tissue had large blood vessels dissected out and was cut into ~100mg explants prior to a 24 hour incubation in phenol free DMEM/F12 with no antibiotics, in glass tubes (VWR) at 37°C. Following incubation media was aliquoted and corresponding explant were stored at -80°C prior to analysis.

Metabolomics

Nuclear magnetic resonance (NMR) based metabolomics provided a non-targeted metabolomics approach. Adipose tissue conditioned media 1 in 4 in NMR buffer (Final concentration: 100 mM sodium phosphate, 500 µM 4,4-dimethyl-4-silapentane-1-sulfonic acid (DSS), 2 mM imidazole and 10% deuterium (D_2O)). Corresponding SC and OM explants

underwent a methanol/water/chlorophorm extraction prior to retention and evaporation of the polar layer. Dried samples reconstituted in 60 µl of 100 mM sodium phosphate buffer containing 100% D_2O and 500 µM DSS. All samples were transferred into 1.7 mm Bruker Sample Jet NMR tubes (Cortecnet, Voisins-Le-Bretonneux, France) via an automatic Gilson. Samples were run on a Bruker 600 MHz Bruker Avance III spectrometer (Bruker Biospin) with a TCl 1.7 mm z-PGF cryogenic probe set at 300K. 1D-^{1}H-NMR spectra were obtained, where spectral width was set to 7,812.5.

1D-^{1}H-NMR spectra were processed using MetaboLab software (57). All 1D data sets were zero-filled to 131,072 data points prior to Fourier Transformation. The chemical shift was calibrated by referencing the DSS signal to 0 p.p.m. 1D-spectra were manually phase corrected. Batch baseline correction was achieved using a spline function. 1D-^{1}H-NMR spectra were exported into Bruker format for metabolite identification and concentration determination using Chenomx 8.2 (Chenomx INC, Edmonton, Canada). All values obtained were normalised to the mass of the appropriate adipose tissue explant. Conditioned media values were made relative to media without adipose tissue. The investigator was blinded to patient type and tissue type during metabolite quantification.

Leptin ELISAs

Leptin was quantified in adipose conditioned media, serum and CSF using the human leptin DuoSet ELISA (DY-398,Bio-techne, Abingdon, UK). ELISA was carried out according to manufacturer's instructions using recommended ancillary kit (Bio-techne, DY008). Conditioned media was diluted 1:50, Serum 1:100 and CSF 1:5 in reagent diluent. Samples were run in duplicate. Total secreted leptin was normalised to corresponding explant mass. Intra-assay variability CV 7.28 %, inter-assay variability CV 8.2% for conditioned media assay. Serum intra-assay variability CV 2.71 % and inter-assay variability CV 6.99 %. CSF yielded intra-assay variability CV 3.85 % and inter-assay variability CV 8.9%.

Statistical analysis

Statistical analysis was performed using Graphpad prism 8 (Graphpad Software Inc, La Jolla, CA, USA) and SPSS 24 (SPSS Inc, Chicago, IL, USA). Data presented as mean ± standard deviation unless otherwise stated. Data normality was assessed by a Shapiro-Wilk normality test. Where data was normally distributed unpaired two-tailed t-tests (equal variance) or Welch's test (unequal variance) were employed, whereas non-parametric data was assessed via Mann-Whitney U. Spearman's rank correlation coefficient (ρ) and Pearson's correlation coefficient (r) was used for assessing correlations in the IIH cohorts. Where data points are missing, data was not imputed. We did not correct for multiple comparisons as this would have increased the likelihood of type II errors with the exception of RNA sequencing data. Results were judged significant at $P<0.05$.

Study approval

IIH subjects were identified from multiple UK centres and samples were collected following informed, written consent. The trials received ethical approval from the York and Humber-Leeds West Research Ethic committee (REC) (13/YH/0366), Dudley local REC (06/Q2702/64) and the Black Country REC (14/WM/0011).

Control patients were recruited via advertisement, where sample collection occurred following informed, written consent. Sample collection was approved by the South Birmingham Local REC and the Black Country REC (14/WM/0011). Control patients for adipose tissue experiments were recruited from elective NHS bariatric surgery lists following written informed consent and was approved by the Black Country REC (14/WM/0011).

Author contributions

AJS designed and conceived the study. CSJW, HFB, ZA, KAM, AY, JLM and CL conducted the experiments. AY, JLM, KAM and AS conducted clinical assessments. CSJW, AY, RS, JLM, KAM and AJS collected clinical samples. CSJW, HFB, ZA, MW, GS, DH, IA analysed the data. CSJW, HFB, IA, SPM, GGL and AJS drafted the manuscript. All authors read the manuscript for intellectual content. All authors have read and approved the final version of the paper.

Acknowledgements

We wish to thank Nicola Crabtree of University Hospitals Birmingham for performing and analysing the DEXA scans.

Funding

This study was funded by the National Institute of Health Research (NIHR) UK (NIHR Clinician Scientist Fellowship (NIHR-CS-011-028) and the Medical Research Council UK (project grant MR/K015184/1 to AJS and a Midlands Neuroscience Teaching and Research Fund grant awarded to CSJW. AJS was awarded a Sir Jules Thorn Award for Biomedical Science. GGL was supported by a Wellcome Trust Senior Research Fellowship (104612/Z/14/Z). IA is funded by RD Lawrence fellowship (Diabetes UK). The views expressed are those of the authors and not necessarily those of the UK National Health Service, the NIHR, or the UK department of Health and Social Care.

Conflict of interest statement

SPM, Invex therapeutics (advisory board and consulting fees 2020). AJS, Invex therapeutics, company director (2019, 2020).

References

1. Mulla Y et al. Headache determines quality of life in idiopathic intracranial hypertension.. *J. Headache Pain* 2015;16:521.

2. Mollan SP, Hoffmann J, Sinclair AJ. Advances in the understanding of headache in idiopathic intracranial hypertension. *Curr. Opin. Neurol.* 2019;32(1):92–98.

3. Mollan SP et al. Idiopathic intracranial hypertension: consensus guidelines on management.. *J. Neurol. Neurosurg. Psychiatry* 2018;89(10):1088–1100.

4. Corbett JJ et al. Visual Loss in Pseudotumor Cerebri: Follow-up of 57 Patients From Five to 41 Years and a Profile of 14 Patients With Permanent Severe Visual Loss. *Arch. Neurol.* 1982;39(8):461–474.

5. Mollan SP, Aguiar M, Evison F, Frew E, Sinclair AJ. The expanding burden of Idiopathic Intracranial Hypertension. *Eye* 2018;1.

6. Adderley NJ et al. Association Between Idiopathic Intracranial Hypertension and Risk of Cardiovascular Diseases in Women in the United Kingdom. *JAMA Neurol.* [published online ahead of print: July 8, 2019]; doi:10.1001/jamaneurol.2019.1812

7. Giuseffi V, Wall M, Siegel PZ, Rojas PB. Symptoms and disease associations in idiopathic intracranial hypertension (pseudotumor cerebri): a case-control study.. *Neurology* 1991;41(2 (Pt 1)):239–44.

8. Hornby C et al. Evaluating the Fat Distribution in Idiopathic Intracranial Hypertension Using Dual-Energy X-ray Absorptiometry Scanning. *Neuro-Ophthalmology* 2018;42(2):99–104.

9. Sinclair AJ et al. Low energy diet and intracranial pressure in women with idiopathic intracranial hypertension: prospective cohort study. *BMJ* 2010;341(jul07 2):c2701–c2701.

10. Mollan SP et al. What are the research priorities for idiopathic intracranial hypertension? A priority setting partnership between patients and healthcare professionals. *BMJ Open* 2019;9(3):e026573.

11. Frič R, Pripp AH, Eide PK. Cardiovascular risk factors in Chiari malformation and idiopathic intracranial hypertension. *Brain Behav.* 2017;7(5):e00677.

551 12. Mani H et al. Diabetes and cardiovascular events in women with polycystic ovary
552 syndrome: a 20-year retrospective cohort study. *Clin. Endocrinol. (Oxf).* 2013;78(6):926–
553 934.
554 13. O'Reilly MW et al. A unique androgen excess signature in idiopathic intracranial
555 hypertension is linked to cerebrospinal fluid dynamics. *JCI Insight* 2019;4(6):e125348.
556 14. O'Reilly MW et al. Serum testosterone, sex hormone-binding globulin and sex-specific
557 risk of incident type 2 diabetes in a retrospective primary care cohort. *Clin. Endocrinol. (Oxf).*
558 2019;90(1):145–154.
559 15. Tabák AG et al. Trajectories of glycaemia, insulin sensitivity, and insulin secretion before
560 diagnosis of type 2 diabetes: an analysis from the Whitehall II study. *Lancet*
561 2009;373(9682):2215–2221.
562 16. Geloneze B et al. HOMA1-IR and HOMA2-IR indexes in identifying insulin resistance
563 and metabolic syndrome: Brazilian Metabolic Syndrome Study (BRAMS).. *Arq. Bras.*
564 *Endocrinol. Metabol.* 2009;53(2):281–7.
565 17. Anderson KM, Odell PM, Wilson PWF, Kannel WB. Cardiovascular disease risk profiles.
566 *Am. Heart J.* 1991;121(1 PART 2):293–298.
567 18. Fujioka S, Matsuzawa Y, Tokunaga K, Tarui S. Contribution of intra-abdominal fat
568 accumulation to the impairment of glucose and lipid metabolism in human obesity.
569 *Metabolism* 1987;36(1):54–59.
570 19. Peiris AN. Adiposity, Fat Distribution, and Cardiovascular Risk. *Ann. Intern. Med.*
571 1989;110(11):867.
572 20. Tomlinson JW et al. Impaired glucose tolerance and insulin resistance are associated
573 with increased adipose 11beta-hydroxysteroid dehydrogenase type 1 expression and
574 elevated hepatic 5alpha-reductase activity.. *Diabetes* 2008;57(10):2652–60.
575 21. Ball AK et al. Elevated cerebrospinal fluid (CSF) leptin in idiopathic intracranial
576 hypertension (IIH): evidence for hypothalamic leptin resistance?. *Clin. Endocrinol. (Oxf).*
577 2009;70(6):863–869.
578 22. Hornby C, Mollan SP, Botfield HF, O'Reilly MW, Sinclair AJ. Metabolic Concepts in

579 Idiopathic Intracranial Hypertension and Their Potential for Therapeutic Intervention. *J.*
580 *Neuro-Ophthalmology* 2018;1.
581 23. Lampl Y et al. Serum leptin level in women with idiopathic intracranial hypertension. *J.*
582 *Neurol. Neurosurg. Psychiatry* 2002;72(5):642–643.
583 24. Dhungana S, Sharrack B, Woodroofe N. Cytokines and chemokines in idiopathic
584 intracranial hypertension. *Headache* 2009;49(2):282–285.
585 25. Behbehani R et al. Is cerebrospinal fluid leptin altered in idiopathic intracranial
586 hypertension?. *Clin. Endocrinol. (Oxf).* 2010;72(6):851–852.
587 26. Samancl B et al. Evidence for potential involvement of pro-inflammatory adipokines in
588 the pathogenesis of idiopathic intracranial hypertension. *Cephalalgia* 2017;37(6):525–531.
589 27. Lönnqvist F et al. Leptin secretion from adipose tissue in women. Relationship to plasma
590 levels and gene expression.. *J. Clin. Invest.* 1997;99(10):2398–404.
591 28. Schwartz MW, Peskind E, Raskind M, Boyko EJ, Porte D. Cerebrospinal fluid leptin
592 levels: Relationship to plasma levels and to adiposity in humans. *Nat. Med.* 1996;2(5):589–
593 593.
594 29. Amitani M, Asakawa A, Amitani H, Inui A. The role of leptin in the control of insulin-
595 glucose axis. *Front. Neurosci.* 2013;7:51.
596 30. Oie S et al. Hepatic rRNA Transcription Regulates High-Fat-Diet-Induced Obesity. *Cell*
597 *Rep.* 2014;7(3):807–820.
598 31. Murayama A et al. Epigenetic Control of rDNA Loci in Response to Intracellular Energy
599 Status. *Cell* 2008;133(4):627–639.
600 32. Grummt I, Ladurner AG. A Metabolic Throttle Regulates the Epigenetic State of rDNA.
601 *Cell* 2008;133(4):577–580.
602 33. Yoshihama M et al. The human ribosomal protein genes: sequencing and comparative
603 analysis of 73 genes.. *Genome Res.* 2002;12(3):379–90.
604 34. Franck N et al. Identification of adipocyte genes regulated by caloric intake. *J. Clin.*
605 *Endocrinol. Metab.* 2011;96(2):E413–E418.
606 35. Crown SB, Marze N, Antoniewicz MR. Catabolism of Branched Chain Amino Acids

607 Contributes Significantly to Synthesis of Odd-Chain and Even-Chain Fatty Acids in 3T3-L1
608 Adipocytes. *PLoS One* 2015;10(12):e0145850.
609 36. Rosenthal J, Angel A, Farkas J. Metabolic fate of leucine: a significant sterol precursor in
610 adipose tissue and muscle. *Am. J. Physiol. Content* 1974;226(2):411–418.
611 37. Tabák AG, Herder C, Rathmann W, Brunner EJ, Kivimäki M. Prediabetes: A high-risk
612 state for diabetes development. *Lancet* 2012;379(9833):2279–2290.
613 38. Malmström R, Taskinen M-R, Karonen S-L, Yki-Järvinen H. Insulin increases plasma
614 leptin concentrations in normal subjects and patients with NIDDM. *Diabetologia*
615 1996;39(8):993–996.
616 39. Segal KR, Landt M, Klein S. Relationship Between Insulin Sensitivity and Plasma Leptin
617 Concentration in Lean and Obese Men. *Diabetes* 1996;45(7):988–991.
618 40. Després JP, Lemieux I. Abdominal obesity and metabolic syndrome. *Nature*
619 2006;444(7121):881–887.
620 41. Ezeh U, Pall M, Mathur R, Azziz R. Association of fat to lean mass ratio with metabolic
621 dysfunction in women with polycystic ovary syndrome. *Hum. Reprod.* 2014;29(7):1508–
622 1517.
623 42. Rotondo F et al. Glycerol is synthesized and secreted by adipocytes to dispose of
624 excess glucose, via glycerogenesis and increased acyl-glycerol turnover. *Sci. Rep.*
625 2017;7(1):1–14.
626 43. Andrews LE, Liu GT, Ko MW. Idiopathic Intracranial Hypertension and Obesity. *Horm.*
627 *Res. Paediatr.* 2014;81(4):217–225.
628 44. Ferrannini E et al. Insulin action and age. European Group for the Study of Insulin
629 Resistance (EGIR).. *Diabetes* 1996;45(7):947–53.
630 45. Herman WH et al. Early detection and treatment of type 2 diabetes reduce
631 cardiovascular morbidity and mortality: A simulation of the results of the Anglo-Danish-Dutch
632 study of intensive treatment in people with screen-detected diabetes in primary care
633 (ADDITION-Europe). *Diabetes Care* 2015;38(8):1449–1455.
634 46. Feldman AL et al. Screening for type 2 diabetes: do screen-detected cases fare better?.

635 *Diabetologia* 2017;60(11):2200–2209.
636 47. Stewart PM, Boulton A, Kumar S, Clark PMS, Shackleton CHL. Cortisol Metabolism in
637 Human Obesity: Impaired Cortisone→Cortisol Conversion in Subjects with Central Adiposity
638 1. *J. Clin. Endocrinol. Metab.* 1999;84(3):1022–1027.
639 48. Galarraga M et al. Adiposoft: automated software for the analysis of white adipose tissue
640 cellularity in histological sections. *J. Lipid Res.* 2012;53(12):2791–2796.
641 49. Martin M. Cutadapt removes adapter sequences from high-throughput sequencing
642 reads. *EMBnet.journal* 2011;17(1):10.
643 50. Dobin A et al. STAR: ultrafast universal RNA-seq aligner. *Bioinformatics* 2013;29(1):15–
644 21.
645 51. Anders S, Pyl PT, Huber W. HTSeq--a Python framework to work with high-throughput
646 sequencing data. *Bioinformatics* 2015;31(2):166–169.
647 52. Dyer NP, Shahrezaei V, Hebenstreit D. LibinorM: An htseq-count analogue with
648 improved normalisation of Smart-seq2 data and library preparation diagnostics. *PeerJ*
649 2019;2019(2):e6222.
650 53. Love MI, Huber W, Anders S. Moderated estimation of fold change and dispersion for
651 RNA-seq data with DESeq2. *Genome Biol.* 2014;15(12):550.
652 54. Lawrence M et al. Software for Computing and Annotating Genomic Ranges. *PLoS*
653 *Comput. Biol.* 2013;9(8):e1003118.
654 55. Akerman I et al. Human Pancreatic β Cell lncRNAs Control Cell-Specific Regulatory
655 Networks.. *Cell Metab.* 2017;25(2):400–411.
656 56. Elhassan YS et al. Nicotinamide Riboside Augments the Aged Human Skeletal Muscle
657 NAD+ Metabolome and Induces Transcriptomic and Anti-inflammatory Signatures. *Cell Rep.*
658 2019;28(7):1717-1728.e6.
659 57. Ludwig C, Gunther UL. MetaboLab - advanced NMR data processing and analysis for
660 metabolomics. *BMC Bioinformatics* 2011;12(1):366.
661

Figures

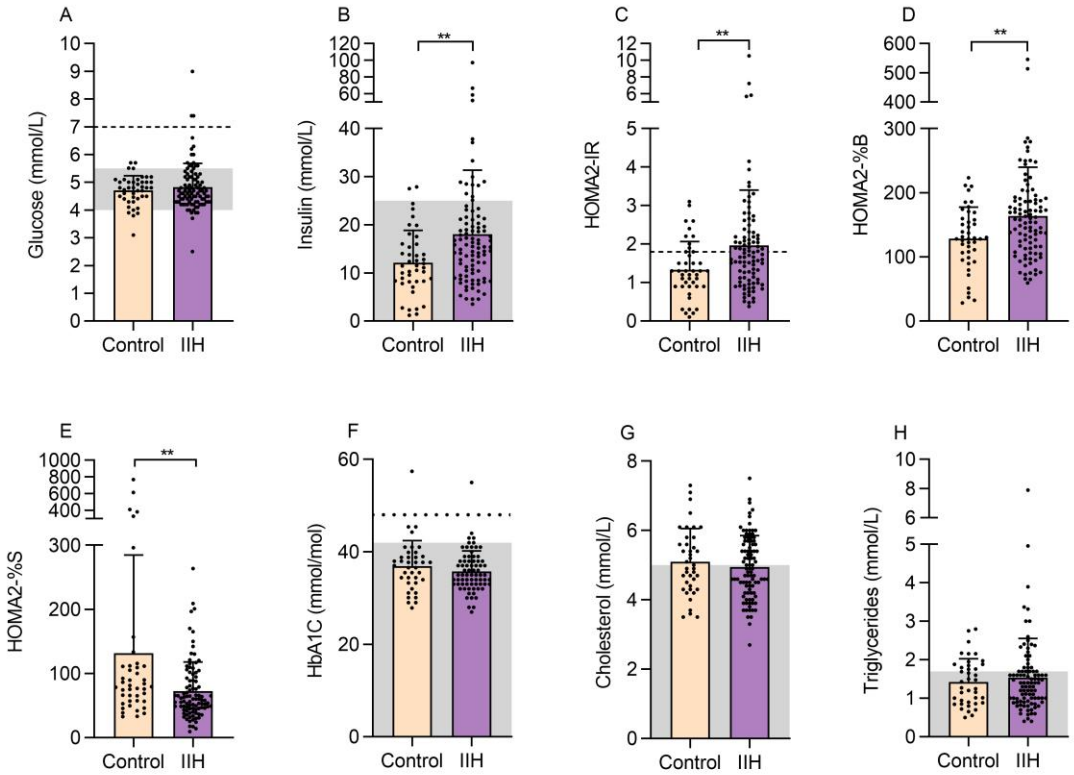

Figure 1) Perturbed metabolic function in IIH

Histograms of fasted glucose (**A**), insulin (**B**), HOMA2-IR (**C**), HOMA2-%B (**D**), HOMA2-%S (**E**), HbA1C (**F**), Cholesterol (**G**) and Triglycerides (**H**) in control (n=43) and IIH patients (n=97). Grey boxes represent healthy clinical reference ranges. A and F dotted lines represent thresholds suggestive of type 2 diabetes mellitus. C dotted line represents HOMA2-IR score 1.8, threshold for insulin resistance. N represents an individual patient. Data presented as mean±SD, **=P<0.01.

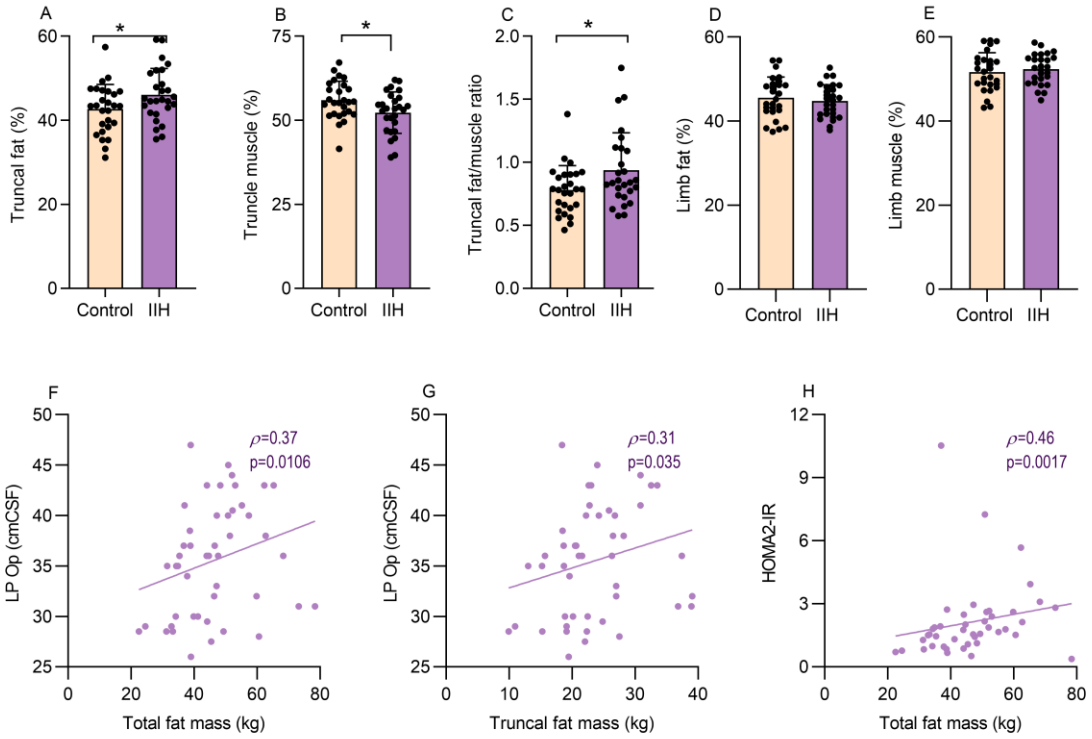

671

672 **Figure 2) IIH patients have an altered body composition**

673 IIH and control patient body composition assessed via dual x-ray absorptiometry (DEXA)
674 scanning. Histograms of (**A**) Truncal fat percentage, (**B**) truncal lean percentage, (**C**) truncal
675 fat/lean ratio, (**D**) limb fat percentage and (**E**) limb lean percentage. A-E, n=27 for control and
676 IIH. Scatter graphs of LP Op vs (**F**) total body fat (n=47) and (**G**) truncal fat mass (n=47), and
677 (**H**) HOMA2-IR vs total fat mass (n=44) in IIH patients. N represents an individual patient.
678 Unpaired t-test for B-D. Manny-Whitney test for A,E. Spearman's correlations for F-H. Data
679 presented as mean±SD. *=p<0.05.

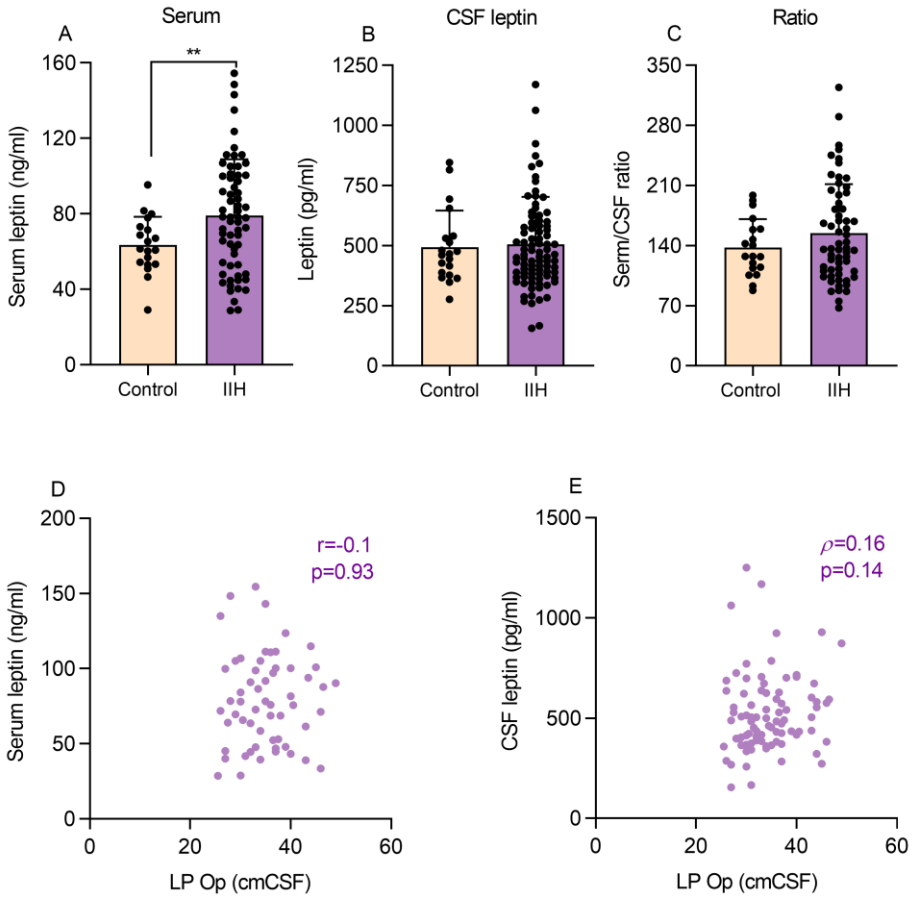

680

681 **Figure 3) IIH patients display an enhanced hyperleptinaemia**

682 Fasted leptin levels assed by ELISA in IIH and control patients. Serum leptin (**A**) in control
683 (n=19) and IIH patients (n=60). CSF leptin in IIH (N=87) and control (N=20) patients (**B**).
684 Serum/CSF ratio in control (n=19) and IIH (n=58) patients (**C**). Scatter graph of lumbar
685 puncture opening pressure (LP Op) vs serum leptin (**D**) and CSF leptin (**E**). N represents an
686 individual patient. Welch's t-test for A and Mann-Whitney test for B and C. Pearson's
687 correlation for D and Spearman's correlation for E. Data presented as mean±SD,**=p<0.01.

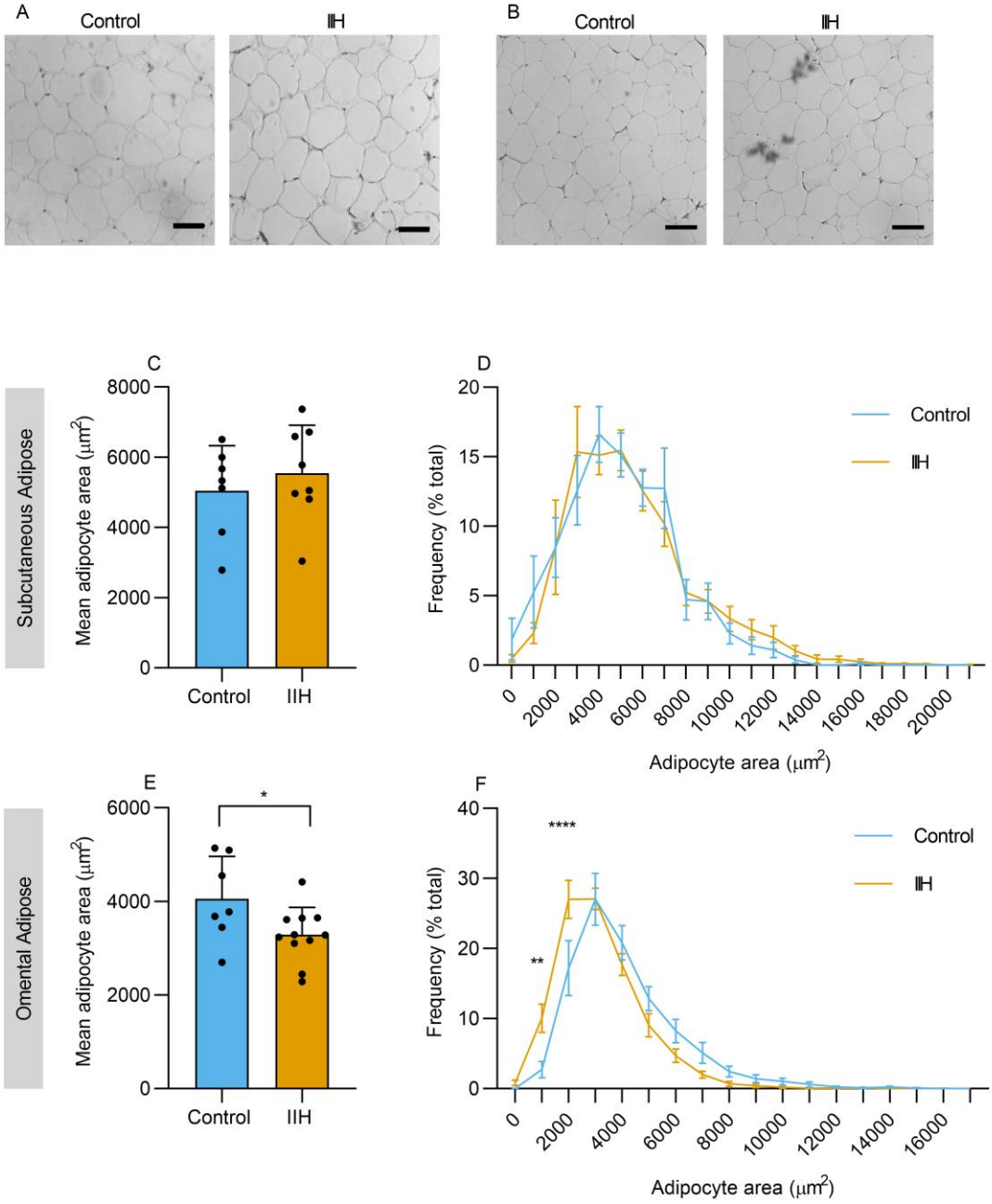

688

689 **Figure 4) Histomorphometric analysis of IIH adipose tissue.**

690 Micrographs of paired paired subcutaneous (SC) (**A**) and omental (OM) (**B**) adipose tissue
691 from age sex and BMI matched control and IIH patients. Mean adipocyte (**C**) and adipocyte
692 area frequency (**D**) SC adipocyte area in control (n=7) and IIH (n=8). Mean OM adipocyte area
693 (**E**) and adipocyte area frequency (**F**) in control (n=7) and IIH (n=11). N represents an
694 individual patient. Scale bar = 100µm . Unpaired t-test for C and E. Two-way ANOVA with

695 Sidaks multiple comparison test for D and F. Data presented as mean±SD for C and E and
696 mean±SEM for D and F, *=p<0.05,*=p<0.01, ****=p<0.0001.

697

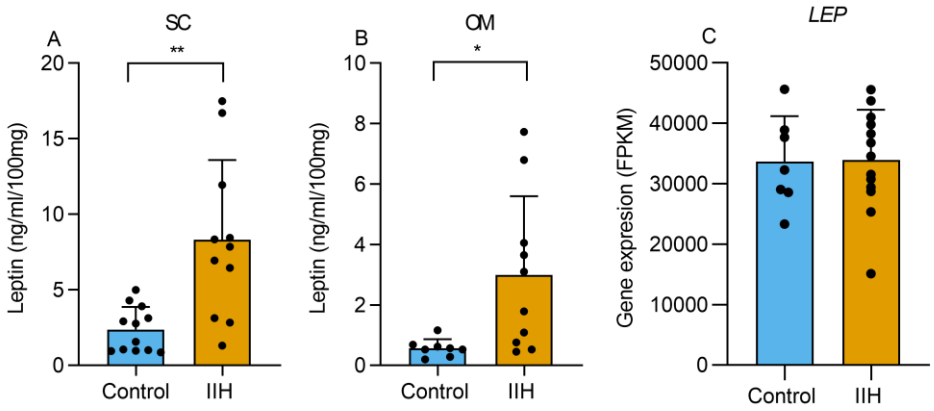

Figure 5) Adipocyte leptin hypersecretion in IIH

Leptin secretion assessed from ex vivo adipose tissue via ELISA in control and IIH patients. (**A**) Leptin secretion from SC adipose tissue in controls (n=12) and IIH (n=11). (**B**) Leptin secretion from OM adipose tissue in controls (n=8) and IIH (n=10). (**C**) *LEP* gene expression in subcutaneous adipose tissue. N represents and individual patient. Welch's t-test for A and B, t-test for C. Data presented as mean±SD, *=P<0.05, **=P<0.01.

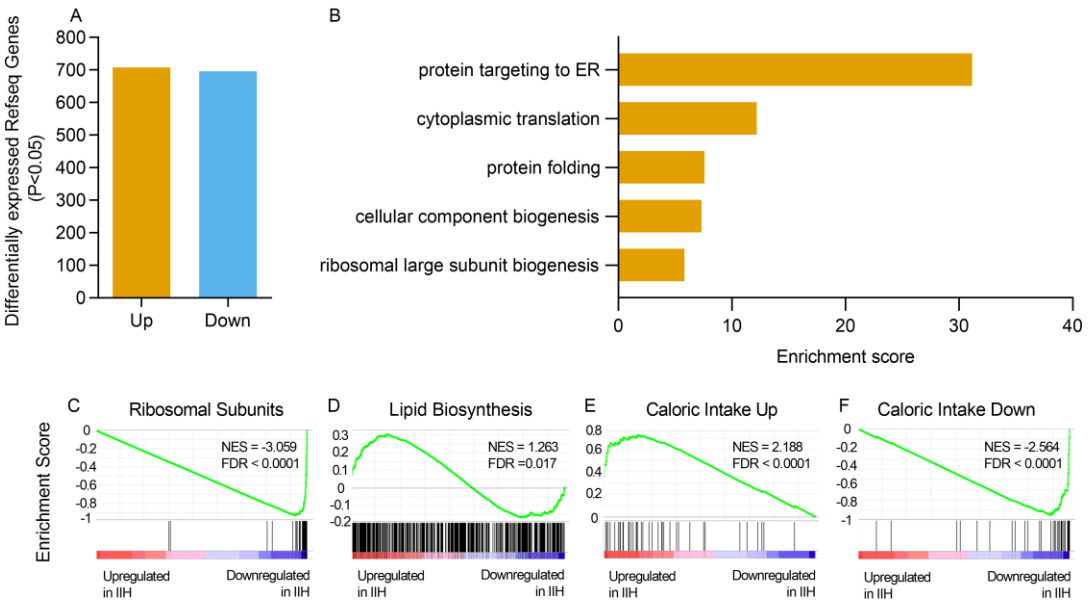

Figure 6) IIH SC adipose tissue displays a distinct transcriptome

Differential gene expression (DGE) analysis of SC adipose tissue from control vs IIH patients. (**A**) Bar plot displaying the number of differentially expressed Refseq genes at p<0.05. (**B**) Gene ontology for significantly downregulated genes in IIH adipose. Gene set enrichment analysis of (**C**) Ribosomal subunits, (**D**) Lipid Biosynthesis, (**E**) Caloric Intake Up and (**F**) Caloric Intake Down against differential expression data from adipose tissue of control vs IIH patients. NES= normalised enrichment score, FDR= False Discovery Rate. The green line represents the accumulation of genes in the indicated gene list against the expression pattern in control vs IIH patients (Blue- downregulated in samples from IIH, red- upregulated in samples from IIH patients). Control N=7, IIH N=13.

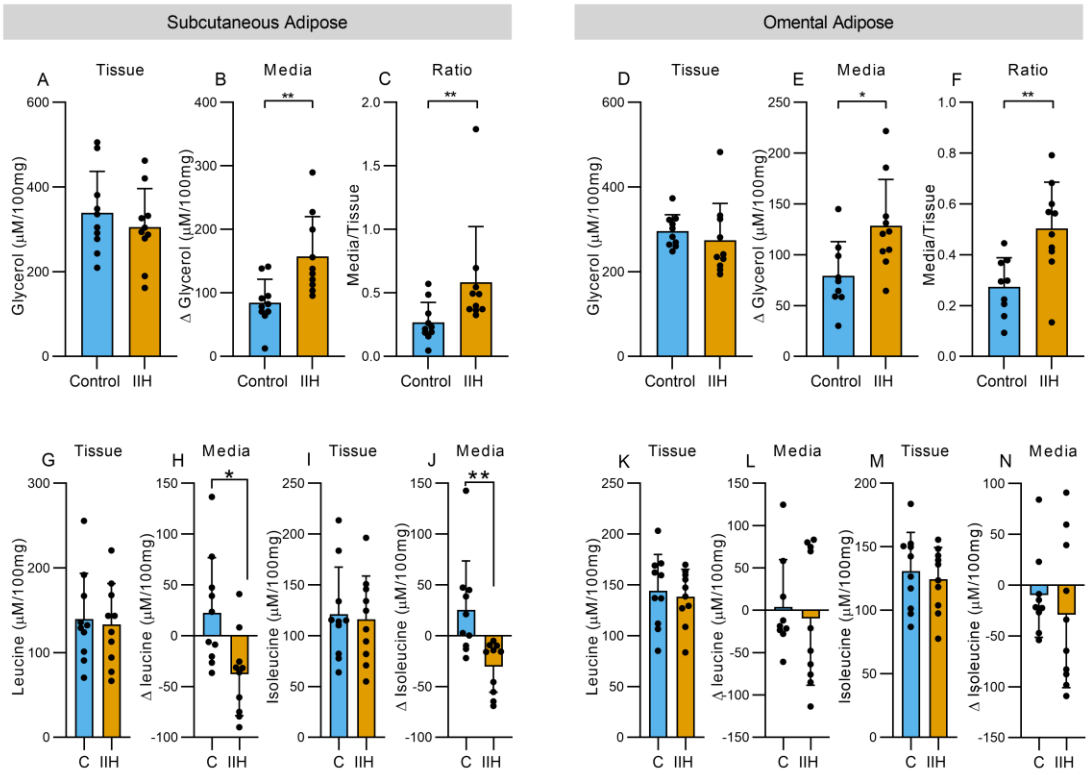

719

720 **Figure 7) IIH adipose displays features of altered lipid metabolism**

721 NMR based metabolomics on paired SC and OM adipose tissue explants and corresponding
722 media in control and IIH patients. Tissue and media levels of glycerol in SC (n=10) (**A-C**) and
723 OM (control n=9, IIH n=10) (**D-F**). Tissue and media levels of leucine and isoleucine in SC (**G-**
724 **J)** and OM (**K-N**) adipose tissue N=10. N represents a single patient's adipose explant or
725 corresponding media. T-tests and Mann-Whitney tests. Data presented as mean±SD,
726 *=P<0.05, **=P<0.01.

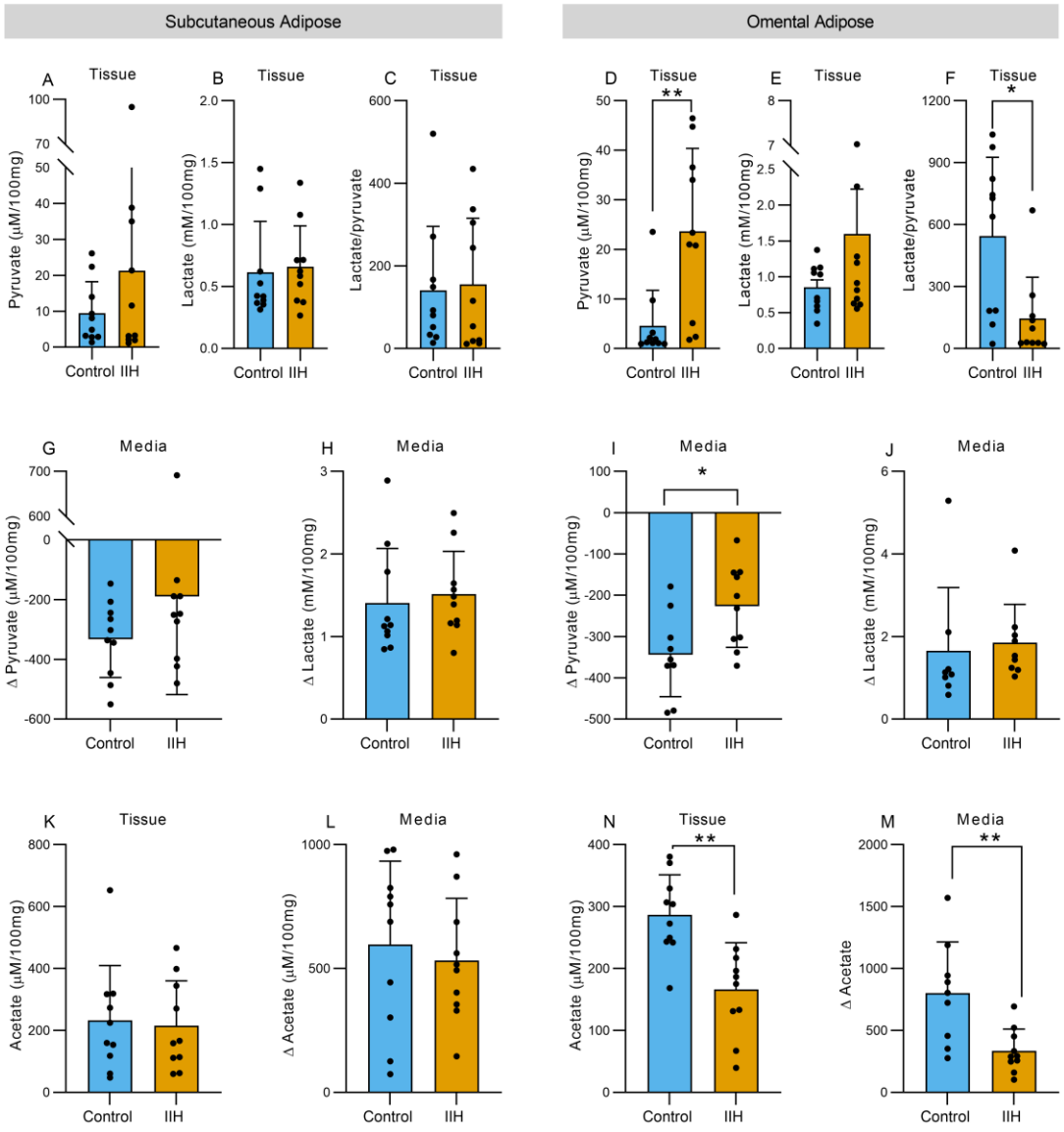

Figure 8) IIH OM adipose tissue displays features of altered nutrient utilisation

NMR based metabolomics on paired SC and OM adipose tissue explants and corresponding media in control and IIH patients. Tissue concentrations of pyruvate, lactate and pyruvate/lactate ratio in SC (**A-C**) and OM (**D-F**) adipose tissue. Media exchange of pyruvate and lactate in SC (**G-H**) and OM (**I-J**). Tissue concentration and media exchange of acetate in SC (**K-L**) and OM (**M-N**) adipose tissue. N represents a single patient's adipose explant or corresponding media. T-tests and Mann-Whitney tests. Data presented as mean±SD, *=P<0.05, **=P<0.01.

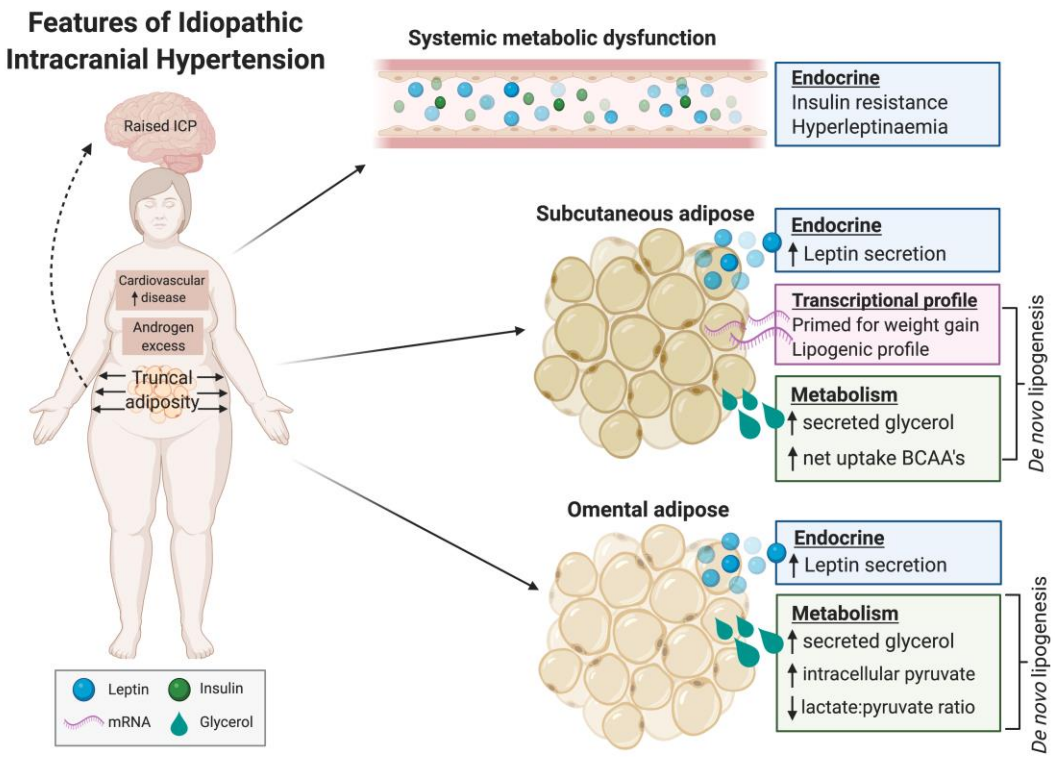

736

737 **Figure 9) IIH metabolism concept figure**

738 IIH patients display systemic and tissue level metabolic disruption in excess to that conferred
739 by obesity. IIH patients are insulin resistant and display hyperleptinaemia, where they have
740 increased abdominal obesity. IIH adipose tissue displays leptin hypersecretion, and features
741 of transcriptomic and metabolic dysfunction.

Tables

Table 1) Characteristics of IIH and control subjects

Characteristics	Control	IIH
Number (N)	43	97
Sex (% female)	100	100
Age (years)	45.5 ± 8.8****	32.4 ± 7.8
BMI (kg/m^2)	39.0 ± 4.5	40.0 ± 6.5
Systolic BP (mmHg)	127.9 ± 18.26	126.4 ± 14.67
Diastolic BP (mmHg)	75.35 ± 10.4	74.86 ± 11.13
LP OP (cmCSF)	N/A	34.8 ± 5.7
Fasting glucose (mmol/L)	4.71 ± 0.53	4.82 ± 0.86
Fasting insulin (mlU/L)	12.1 ± 6.7**	18.1 ± 13.3
HOMA2-IR	1.33 ± 0.74**	1.97 ± 1.44
HOMA2-%B	128.6 ± 48.7**	163.6 ± 76.4
HOMA2-%S	131.6 ± 153.3**	72.4 ± 45.5
HbA1c	36.8 ± 5.5	35.8 ± 4.4
Cholesterol	5.10 ± 0.96	4.94 ± 0.91
Triglycerides	1.42 ± 0.61	1.54 ± 1.01
Sub study 1: Hepatic and renal profile		
Number (N)	25	14
Age (years)	41.6 ± 4.9	39.3 ± 6.8
BMI (kg/m^2)	35.5 ± 3.5	36.7 ± 6.0
ALP (U/L)	117 ± 34.5*	160.2 ± 57.0
LP OP (cmCSF)	N/A	36.7±4.2
AST (U/L)	16.4 ± 6.4	20.5 ± 7.5
Bilirubin (U/L)	4.4 ± 2.8**	7.6 ± 4.0
Urea (mmol/l)	4.04±0.95	3.99±0.73
Creatinine (µmol/L)	81.5±5.6**	88.3±6.4
eGFR (ml/min/1.73m^2)	77.38±7.35*	71.44±7.4
Sub study 2: DEXA profile		
Number	27	27
Age (years)	39.5 ± 4.9	37.2 ± 5.1
BMI (kg/m^2)	35.0 ± 4.4	36.8 ± 7.2
LP OP (cmCSF)	N/A	34.8±5.2
Total fat (kg)	40.2 ± 10.2	42.7 ± 11.6
Truncal fat (kg)	20.1 ± 5.9	22.4 ± 7.4
Limb fat (kg)	19.3 ± 4.7	19.3 ± 5.2
Total lean (kg)	50.1 ± 6.7	49.3 ± 7.7
Truncal lean (kg)	25.7 ± 3.4	24.0 ± 4.2
Limb lean (kg)	21.6 ± 3.4	22.2 ± 3.8
Total bone (kg)	1.79 ± 0.29*	1.99 ± 0.30
Truncal bone (kg)	0.63 ± 0.12***	0.76 ± 0.15
Limb bone (kg)	1.16 ± 0.20	1.21 ± 0.18

BMI= Body mass index, BP= Blood pressure, LP OP= Lumbar puncture opening pressure, HOMA2-IR= Homeostatic model assessment 2- Insulin resistance, HOMA2-%B= HOMA- beta cell function, HOMA2-%S= HOMA- Insulin sensitivity, HbA1c = Glycated haemoglobin, ALP= Alkaline phosphatase, AST= Aspartate transaminase, eGFR= estimated glomerular filtration rate. Data presented as mean ± SD. *=p<0.05, **=p<0.01, ***=p<0.001 and ****=p<0.0001.